Archaeol Anthropol Sci (2019) 11:15–31
DOI 10.1007/s12520-017-0530-5

ORIGINAL PAPER

Investigation of early Bronze Age civilizations in Yunnan: a scientific analysis of metallurgical relics found at the Guangfentou ruins in Jiangchuan

Guisen Zou[1] · Jianfeng Cui[2] · Xu Liu[3] · Xiaorui Li[3] · Rui Min[3]

Received: 14 February 2017 / Accepted: 16 July 2017 / Published online: 31 July 2017

Abstract We herein report on an examination of the compositions of copper relics unearthed from the Guangfentou site in Jiangchuan, Yunnan, China. Scanning electron microscopy combined with energy-dispersive X-ray spectroscopy (SED-EDS), metallographic microscopy, and lead isotope ratio analysis were used to analyze 20 metallurgical relics. The results indicated that the relics were either copper metal or copper slag. The copper metal was composed of either metallic copper or tin bronze, while the copper slags were either smelting slag or melting slag, with the melting slags being composed of refining or alloying slag. The Guangfentou site in the Jiangchuan county contains an extraordinarily complete set of bronze metallurgical relics from the Bronze Age of Yunnan. The processes involved in this site include smelting of sulfidic ores, refining of primary raw copper, bronze alloying, and bronze casting. This was an important metallurgical site in the ancient Dian Kingdom and has provided clues that will aid in efforts to reveal the origins of bronze smelting technologies and the sources of the copper ores used by the ancient Dian civilization.

Keywords Archaeometallurgy · Guangfentou site · Copper slags · Bronze culture · Dian Kingdom

✉ Jianfeng Cui
cuijianfeng@pku.edu.cn

[1] Institute for Cultural Heritage and History of Science and Technology, University of Science and Technology Beijing, Beijing 100083, China

[2] School of Archaeology and Museology, Peking University, Beijing 100871, China

[3] Yunnan Provincial Institute of Cultural Relics and Archaeology, Kunming 650118, China

Introduction

Yunnan lies on the southwest border of China and is rich in mineral resources. This region gave rise to and sustained a flourishing Bronze Age civilization, and so, large numbers of exquisite bronze artifacts have been unearthed there, providing a historical view of the products and quotidian routines of the society during that period. These bronze artifacts are artistic treasures and are richly infused with the ethnic and local characteristics of China's Bronze Age civilizations (Zhang 1989).

The ancient Dian culture, which acts as an important part of the ancient Yunnan bronze culture, is a bronze culture in Central Yunnan, China, which dates from the Warring States Period to the Eastern Han Dynasty. Its bronzes are unique and different from the Central Plains culture in terms of vessel shapes and ornamentation, for example. The Dian culture produced a number of sacrificial vessels, including bronze drums and bronze shell storage containers, which differ from that of the ritual system of the Central Plains. To date, over 500 pieces of bronzeware have been analyzed for the Dian culture (Cui and Wu 2008). According to the data available, the characteristics of bronze craftsmanship of the Dian culture can be summarized. For example, in terms of the alloy ratios employed, the weapons, farm tools, and decorations are mainly composed of tin bronze alloys and pure copper and are essentially free from lead. During the early period, bronze drums, shell storage containers, and other large-scale objects were produced mainly from tin bronze alloys; however, large quantities of lead were used from the beginning of the middle period. In terms of the craftsmanship, weapons and farm tools were molded by hot forging, while large objects, animal patterns, and buckles were molded by casting, and both hot tinning and gilding technologies were widely employed. Similar technologies were also utilized in the culture of the southwestern aborigines, creating a unique system that differed from that of the Central Plains and the South and the Northern Grassland (Di Qiang) during the same period. From the archeological data of the Dian culture, we can see that large-scale cemeteries were explored (i.e., Lijiashan of Jiangchuan, Shizhaishan of Jinning, Yangfutou of Kunming, Taijishan of Anning, and Shibeicun of Chenggong), and the larger sites, namely Lijiashan of Jiangchuan and Shizhaishan of Jinning, were considered cemeteries of the Dian Kingdom. However, to date, studies into the origin of Yunnan archeology have focused on burials close to the Dianchi Lake, while the habitations received little or no attention (Allard 1998.)

To date, large numbers of ancient Yunnan bronze artifacts have been unearthed, and a number of smelting sites have been discovered (see Fig. 1), including the Wasezhen site (Li and Han 2011), Citongguan site (Yang 2010), Chongzipi site (Wang et al. 1997), Longbohe site (Yang 2010), Shijiazhai site (Qi 2014), Yubeidi site (Jiang and Zhu 2014), Xingyi site (Qiu 2015), Wangjiadun site (Zhang 2000), and Yinsuodao site (Min 2009). Of these sites, only the Citongguan site in Yuxi, Chongzipi smelting site in Gejiu, and Shijiazhai smelting site in Jinping had been investigated, and no complete set of metallurgical relics from the Yunnan Bronze Age has been discovered thus far. Our investigation and analysis of Yunnan Bronze Age metallurgical relics are therefore of great significance and have important implications for research regarding the origin and development of the Yunnan Bronze Age civilization.

Archeological background of the Guangfentou ruins

The Guangfentou site is located on Guangfentou mountain of Luju town, which is within the Jiangchuan district in the Yunnan province. It is one of the few archeometallurgical sites from the Dian civilization period to be discovered thus far. Indeed, it was discovered approximately 2 km north of the south coast of the Fuxian Lake Highlands during a survey conducted in March 1984. To learn more about the nature of smelting in the Dian civilization, the Yunnan Provincial Institute of Cultural Relics and Archaeology, the Peking University School of Archeology and Museology, the Yuxi Antique Management Office, and the Jiangchuan Cultural Relic Management Office performed a two-stage archeological excavation from November 2011 to June 2012. The area of the excavation site was approximately 600 m^2, and it was confirmed that the area of the Guangfentou site is around 170,000 m^2. In addition, the thickest cultural layer measured 5.2 m, and the number of stacking layers reached a maximum of 17. Upon exploration of 26 semi-cryptous housing ruins, 30 ash pits, and 11 building-related activity areas, various relics were unearthed, which were mainly pottery-based items. For example, small Zimukou bowls, plates patterned with concentric circles,

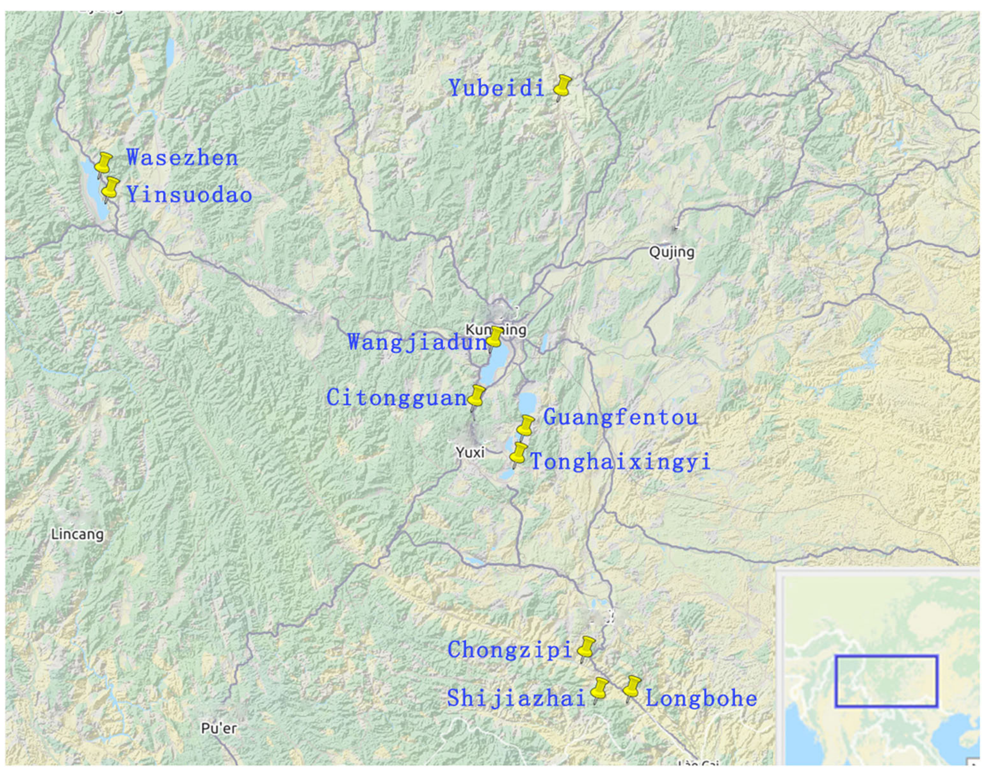

Fig. 1 Map showing the locations of the Yunnan smelting sites

kettles, tanks, pots, and circular plates were discovered. Relics composed of stone, bone, horn, mussels, and jade were also unearthed, and more than 400 samples of copper slag, flotation soil, and sediment were recovered. In the early layers, the number of pottery fragments discovered was higher, and the early cultural period from the eastern Zhou dynasty to the western Han dynasty was judged from the characteristics of the pottery and the stacking relationships between the layers. The late period was likely associated with the Ming and Qing dynasties.

Based on the combination of objects and stratigraphic stacking, the early cultural layer was divided into three stages. In the first stage, relics were found mainly on the top of the Guangfentou mountain, where red pottery blending sand and semi-cryptic-type sites were characteristic. In the second stage, a large quantity of red clay pottery was discovered, in addition to weapons and tools composed of bronze, such as arrowheads, chisels, claw sickles, buckles, belt hooks, and fish hooks. In addition, house sites and huge ash pits were observed, located at the top of the site and in the northwest of the platform edge. The ash pits were mostly rounded, with diameters of 1–1.5 m and depths of 1.2–1.4 m, and these pits could be divided into three or four layers. Large quantities of slags were also found in this stage. In the third stage, a new shape of plates appeared, namely small and shallow plates bearing an arced pattern. Small amounts of bronze were also detected in this stage. Furthermore, only one house site and one ash pit were found, located on the west top of the site. This house was essentially the same as that in the first stage (Li 2016) (see Figs. 2, 3, and 4).

During the excavation, sporadic copper slags were found in the early and late cultural layers, and stone molds were also discovered. All the samples examined herein belong to the ancient Dian culture, as this site appears to be located in a central region within the Dian civilization. Research on its metallurgical relics will therefore be expected to identify the nature of the smelting sites and provide important clues for research into the Dian civilization.


Fig. 2 Site of house no. 24


Fig. 3 One of the excavated areas

Materials and Methods

Samples

Twenty metallurgical relics from the Guangfentou site were selected for this study. Photographs of these relics are shown in Fig. 5.

Analytical methods

A cutting machine was used to remove a small fragment from each sample, which was then cold-mounted in epoxy resin. After the epoxy resin had solidified, a precision cutting machine was used to expose a cross section of the sample, which was subsequently sanded using coarse sandpaper followed by fine sandpaper. Finally, the sample was polished using a polishing machine.

In terms of metallographic observations, polished copper blocks were etched using a 4 vol% nitric acid/ethanol solution, and a Nikon ECLIPSE LV100N POL microscope was used for observation alongside a Nikon NIS-Elements D optical microstructure analysis system. The latter was employed to obtain metallographic images.

Scanning electron microscopy coupled with energy-dispersive spectroscopy (SEM-EDS) was used to probe the compositions of the slag samples. A HITACHI TM3030 SEM and a BRUKER Quantax70 spectrometer with an accelerating voltage of 15 kV were used. Sample compositions were determined using a standardless SEM-EDS, and cross-

Fig. 4 Pottery unearthed from the Guangfentou site

sectional analyses were performed based on sample conditions; scans of 90 s were used for all measurements.

Lead isotope analysis (LIA) experiments were carried out in the Orogenic Belts and Crustal Evolution Laboratory, in the School of Earth and Space Science at Peking University. A VG Elemental multicollector–inductively coupled plasma mass spectrometer (MC-ICP-MS) was used to perform the measurements. The relative errors of the $^{207}Pb/^{206}Pb$, $^{208}Pb/^{206}Pb$, and $^{206}Pb/^{204}Pb$ ratios were <0.01, 0.01, and 0.1%, respectively. A solution of the SRM981 international lead isotope standard was used to calibrate the spectrometer, and the standard was remeasured after every set of 6–8 sample measurements.

Analytical results and discussion

As slags are remnants of smelting activities, they contain vast amounts of information regarding smelting processes. The examination of slags can therefore determine the nature of

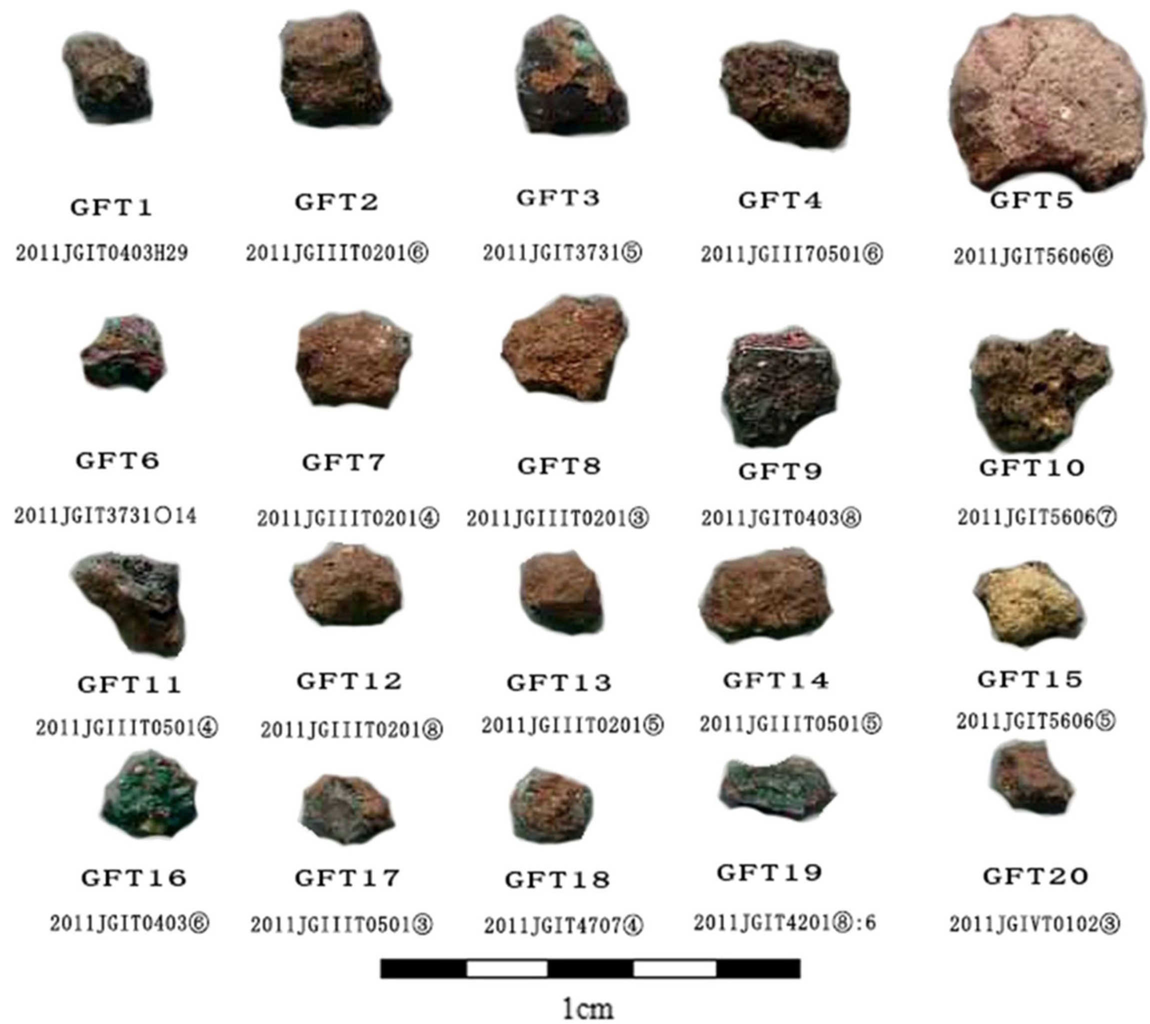

Fig. 5 Photographic images of the samples obtained from the Guangfentou site

the site from which they were obtained and the technological level of the metallurgical processes employed in their preparation. Usually, smelting slags (regardless of whether they stem from the smelting of iron or copper sulfide ores) contain veinstones composed of metals or calcium compounds that are mixed with the ores. The latter slags are primarily composed of fayalite (iron silicates) and wollastonite (calcium silicates). In contrast, melting slags consist primarily of complex silicates composed of silicon and aluminum oxides but may also contain compounds that are formed through interactions with the walls of the furnace (Li 2007) (Table 1).

Smelting

In the backscattered electron (BSE) image of the GFT1 sample (see Fig. 6a), area A was found to be composed mainly of wüstite, while a significant number of white matte and cuprite particles were present out of this area. In addition, in the matrix, large quantities of magnetite were present, small fayalite particles were observed, and a significant number of white matte and cuprite particles were present. Thus, the presence of both cuprite and magnetite indicates that the slag was formed in a strong oxidizing atmosphere. In addition, the conversion of Cu–S into cuprite (Fig. 6b) indicated desulfurization processes, while the removal of iron from the matte (Fig. 6c) resulted in the generation of wüstite and fayalite.

As shown in the BSE images of GFT2 sample (Fig. 7), significant quantities of magnetite and fayalite were present in the matrix, although the fayalite particles were extremely small. The prills were mainly composed of chalcocite (Cu_2S), and small quantities of copper oxide and copper particles were also observed.

As shown in Fig. 8, analysis by polarized optical microscopy (POM) reveals that many cuprous oxides and copper sulfide prills were distributed within GFT10, while a relatively large portion of bornite was also present in the middle section. In addition, the area close to point A contained fayalite formations and widely dispersed metallic copper prills, where many fine lead prills were present among the metallic copper. Significant quantities of wüstite and magnetite were also present in the matrix. Furthermore, as shown in Fig. 8c, copper drops were surrounded by chalcocite, while the rim of the prill was composed of chalcocite, and the inside was cuprite. Moreover, the dislodging of iron from the iron-rich copper is shown (Fig. 8c), where the lightly colored sections represent cuprite, the light gray color represents iron-rich copper, and the gray color represents magnetite.

Finally, the BES image of GFT14 shown in Fig. 9 indicates that the sample matrix contained a relatively high iron content but a low copper content. In addition, large quantities of wüstite were distributed in the matrix, and tin bronze prills were also observed, containing 1.5–4.4% bronze. As tin was not detected in the matrix by SEM-EDS, this indicates the presence of a reducing atmosphere. In the presence of smelting copper ores with noticeable tin contents, the reduction of tin is favored in the presence of copper. It was therefore apparent that this sample was derived from smelting mixed tin–copper ore.

The presence of magnetite in a number of the samples suggests the presence of an oxidizing atmosphere in the reduction furnace (Hohlmann 1997). For example, large quantities of magnetite were detected in the matrices of GFT1, GFT2, and GFT10. In addition, the presence of both magnetite and cuprite in the GFT1 sample indicates that the slag was formed under strongly oxidizing conditions. However, the presence of copper prill also indicates the presence of reducing conditions.

Table 1 Compositional analyses of the smelting slag matrices as determined by the SEM-EDS area analysis

Number	Scanned area	wt%										
		MgO	Al_2O_3	SiO_2	SO_3	K_2O	CaO	TiO	P_2O_5	FeO	CuO	SnO_2
GFT1	Section 1	0.7	7.5	35.5	0.6	1.1	11.0	0.4	3.0	34.5	5.8	n.d.
	Section 2	n.d.	7.7	38.3	n.d.	1.0	11.7	n.d.	3.3	33.0	5.1	n.d.
GFT2	Section 1	n.d.	4.8	26.5	0.5	0.8	5.3	n.d.	1.4	59.1	1.7	n.d.
	Section 2	n.d.	4.5	27.2	0.3	0.7	4.5	0.2	1.3	59.9	1.4	n.d.
GFT10	Section 1	1.2	5.3	26.3	n.d.	0.8	11.4	0.5	3.4	35.0	16.0	n.d.
	Section 2	0.6	5.3	23.2	n.d.	1.6	5.6	0.4	1.3	46.8	15.2	n.d.
	Section 3	n.d.	7.5	23.0	1.2	0.7	5.7	n.d.	1.8	38.1	22.1	n.d.
GFT14	Section 1	1.3	2.5	20.6	n.d.	1.6	12.3	n.d.	3.4	58.3	n.d.	n.d.
	Section 2	1.1	2.5	20.2	n.d.	1.5	10.9	n.d.	3.0	57.4	3.5	n.d.

Data is presented in weight percent, normalized to 100

n.d. not detected

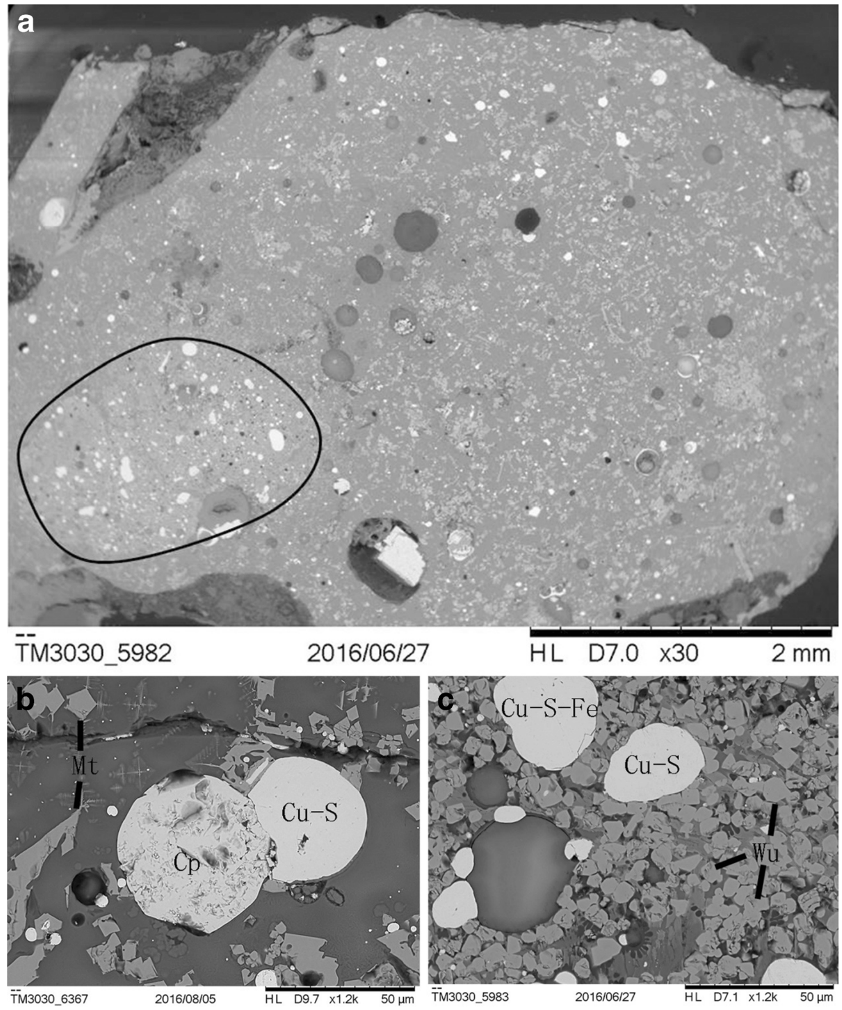

Fig. 6 BES images of GFT1 sample. showing that:**a**, the whole view BES image of the sample, the circle section content much wüstite;**b**, Cp=cuprite, Mt=magenite;**c**, Wu= wüstite

Ryndina previously analyzed the slag of northeastern Balkan Eneolithic culture from a site that employs sulfide ore mixed with oxide ores (Ryndina et al. 1999). Prior to smelting, the sulfide ores would have been roasted under oxidizing conditions to remove any sulfur (Bachmann 1982; Tylecote 1982), and a subsequent increase in temperature to 300–400 °C resulted in burning of the sulfur to either remove sulfur or to convert the sulfides into oxides according to the following reaction (Avetisyan 1954):

$$2MeS + 3O_2 \rightarrow 2MeO + 2SO_2, \mathit{where}\ Me = \mathit{metal}.$$

In addition, ore oxides, such as malachite, dissociate to produce CuO, H_2O, and CO_2:

$$CuCO_3(OH)_2 \rightarrow 2CuO + CO_2 + H_2O\ (< 500^oC)\ (\mathit{Bachmann}\ 1982)$$

If the reaction does not reach completion, the ore will contain CuO, Cu_2O, FeO, FeS, and Cu_2S. Furthermore, at temperatures up to 1150–1200 °C, the reducing conditions of the atmosphere will result in the production of metallic copper (Ryndina et al. 1999):

$$2CuO + Cu_2S \rightarrow 4Cu + SO_2$$
$$2Cu2O + Cu2S \rightarrow 6Cu + SO_2$$
$$2CuO + C \rightarrow 2Cu + CO_2$$
$$2Cu_2O + C \rightarrow 4Cu + CO_2$$

Moreover, at 1150–1250 °C, liquid fayalitic slags form (Tylecote 1980). Indeed, in the GFT1 sample, small quantities of elongated lath-shaped fayalite crystals are present, indicating a fast cooling process. The presence of copper prills, other sulfides (i.e., chalcocite, covellite, and matte), and oxides (i.e., FeO, cuprise, and magnetite) in the matrix suggests that the reducing reaction took place for only a short time. As such, it appears that the mines from which GFT1 is obtained contain mostly sulfide ore coexisting with oxide ores, where the ores were roasted in the oxidizing atmosphere prior to smelting under reducing conditions. Smelting of oxide copper ores containing sulfide impurities resulted in slags with matte (Hanning et al. 2010).

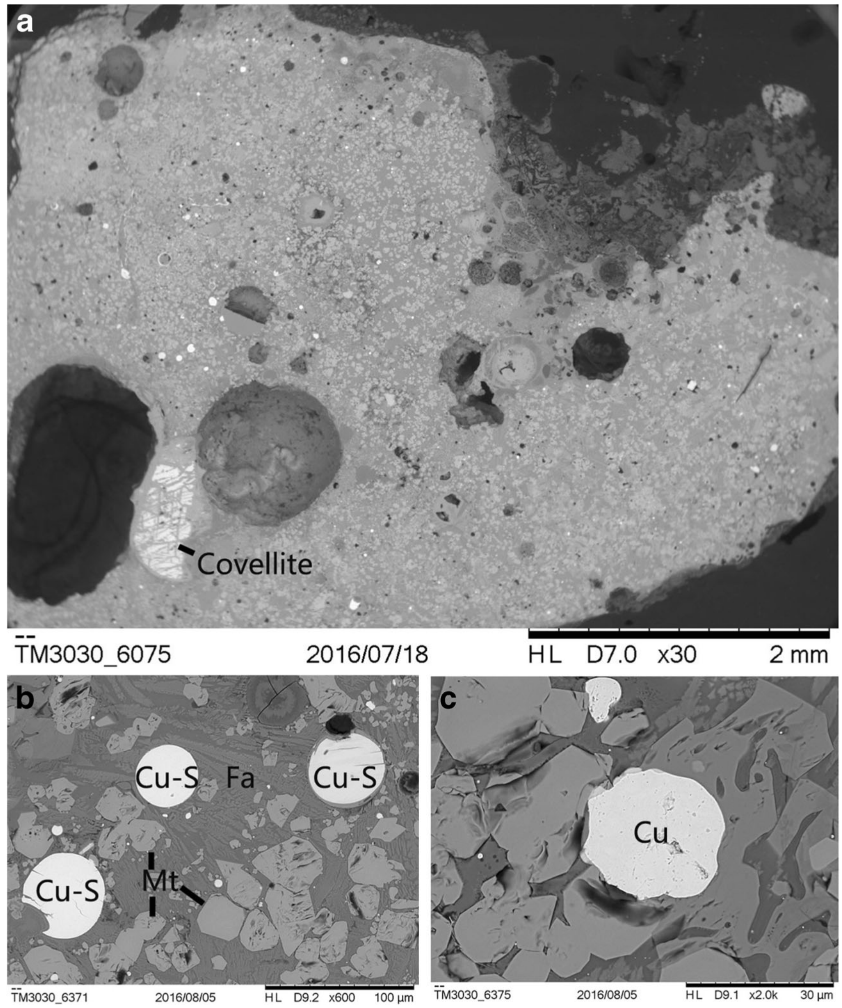

Fig. 7 BES images of GFT2 sample. showing that:**a**, the whole view BES image of the sample, there is a covellite in the slag;**b**, Fa=fayalite, Ma=magenite;**c**, a copper prill

In 1995, Li and Hong (1995) studied the ancient Chinese copper slags and reported that no FeS was present in the reduction slags, and Cu and Cu_2O were not present in the matte slags. In addition, the GFT2 sample contains significant quantities of both chalcocite and copper prills, and so, it is difficult to determine which type of ore or process was used; however, the presence of covellite in the slag may suggest that it originated from a secondary sulfide ore.

In GFT10, point A (see Fig. 8) contains different phases from other areas, as the copper prills contain significantly finer lead prills but very little sulfur. This composition may therefore arise from other smelting processes. In addition, the slag contains large quantities of cuprite, which arises from both Cu_2S and Cu–Fe (FeO is also formed), indicating the presence of a particularly strong oxidizing atmosphere. In addition, the presence of bornite may suggest roasting of the ore.

The smelting process that produced the GFT1 and GFT10 samples therefore appears to have been significantly less efficient. Consequently, large metal-containing phases and unreacted ore remnants remained entrapped in the liquefied slag matrix (Hauptmann 2003). In contrast, the processes that produced the GFT2 and GFT14 samples were more efficient, as indicated by the lower copper contents in the matrices and the lower numbers of copper prills.

From the above analysis, it is apparent that both the site smelting technologies and the ore sources are diverse. This may reflect the technical differences in the different stages employed by the ancient Dian culture, as all samples originate from this period. From the stratigraphic analysis, we concluded that GFT2 was produced earlier than GFT14, but later than GFT10, while GFT1 was excavated from an ash pit. It was not possible to determine exactly which stratum this sample originated from, but the phases and copper contents observed indicate the use of early-stage copper metallurgy technology.

Although smelting sites tend to produce large amounts of slags, we examined only four smelting slags, as the other samples are melting slags. This may be due to random variation through sample selection, although it is also possible that the zones in which smelting and melting were performed were separated from one another, and so, the excavation may not

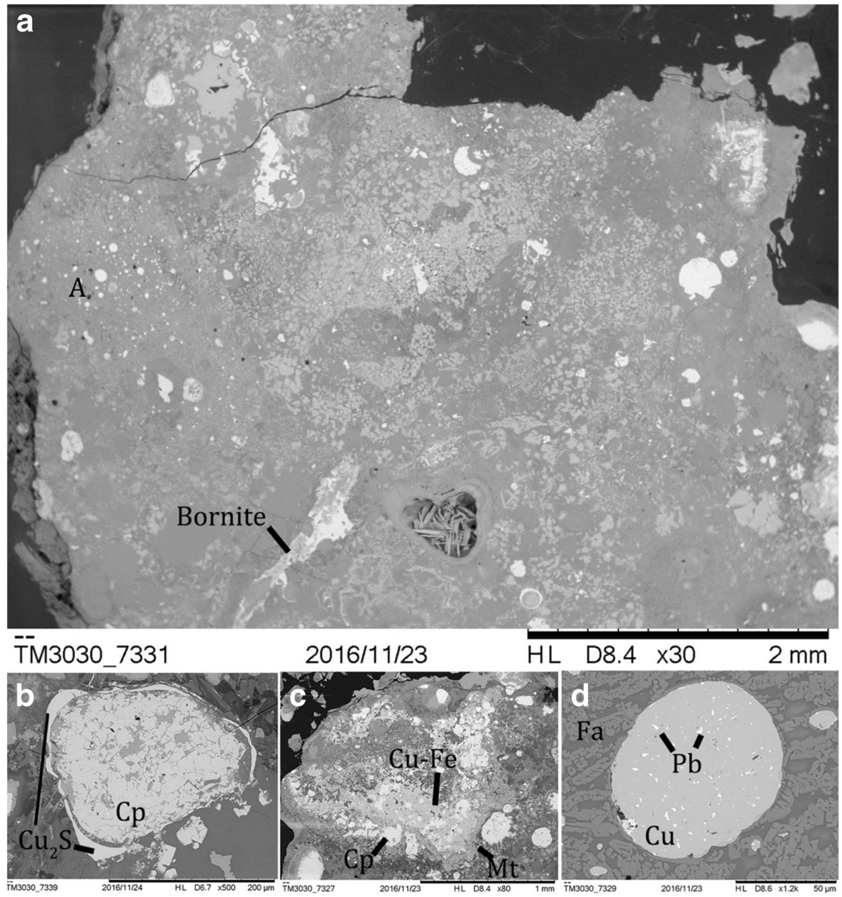

Fig. 8 BES images of GFT10 sample. showing that:**a**, the whole view BES image of the sample, there is a bornite in the slag;**b**, Cp=cuprite, Mt=magenite;**c**, Cp=cuprite, Mt=magenite;**d**, Fa= fayalite

have reached the core zones where smelting was performed. Therefore, further analytical studies of smelting slags are required. A copper mine approximately 3 km from the site may have been used to provide mineral ores for smelting, and so, this mine will be subject to further investigation.

Refining

The compositional analyses of GFT13 slag from the Guangfentou site is shown in Table 2.

The term "refining" refers to the remelting of primary raw metals under an oxidizing atmosphere to induce the oxidation of iron into fayalite and wüstite and thus lower the iron content (Tylecote and Boydell 1978). In the case of the GFT13 sample, POM observations did not detect any sulfides, although large quantities of needle-shaped delafossite and magnetite were observed throughout the sample. As indicated in Fig. 10, the left-hand side of the sample contains copper–iron compounds and cuprous oxide, while the right-hand side consists primarily of metallic copper prills and copper–iron compounds, and the middle section contains regularly shaped needle-like delafossite remnants (Fig. 10d). Preliminary analysis suggests that this composition corresponds to the post-corrosion morphology of the slag. In addition, the middle, left-

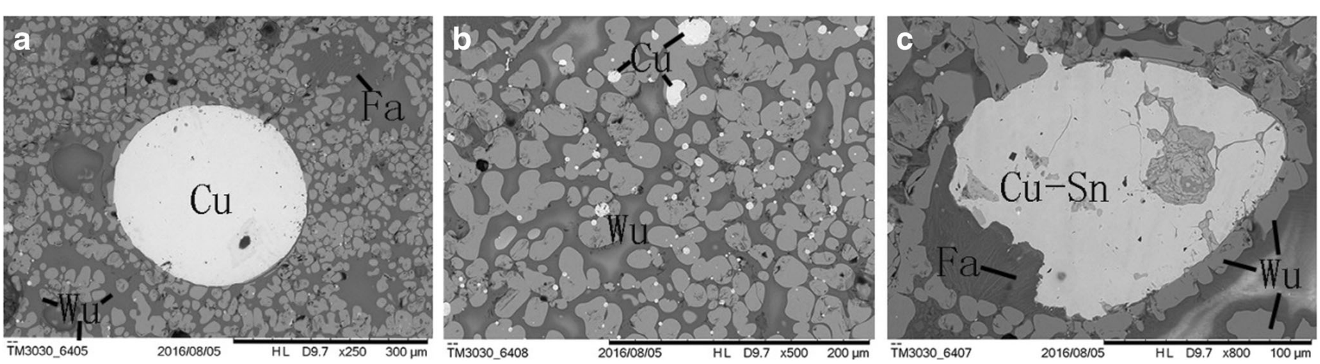

Fig. 9 BES images of GFT14 sample.showing that:**a**, Wu= wüstite, Fa=fayalite;**b**, Wu= wüstite;**c**, Wu=wüstite, Fa=fayalite

Table 2 Compositional analyses of GFT13 refining slag matrices as determined by the SEM-EDS area analysis

Number	Scanned area	wt%										
		MgO	Al_2O_3	SiO_2	SO_3	K_2O	CaO	TiO	P_2O_5	FeO	CuO	SnO_2
GFT13	Left-hand area	1.1	9.2	31.0	n.d.	1.8	10.7	0.9	0.5	15.5	29.4	n.d.
	Middle area	n.d.	n.d.	39.8	n.d.	n.d.	2.0	n.d.	2.6	n.d.	55.7	n.d.
	Right-hand area	1.8	8.2	31.3	0.4	1.4	18.1	n.d.	1.2	21.9	15.6	n.d.

Data is presented in weight percent, normalized to 100

n.d. not detected

hand, and right-hand portions of the slag appear to be parts of a single body, and the outer layer of the middle section is also surrounded by a layer of slag. When such slags are buried, environmental effects cause their chemical components and compositions to change, thereby accounting for the different composition of the middle section of the sample.

Sample GFT13 (Fig. 10) is an example of a refining slag. Although magnetite is a particularly common phase in copper

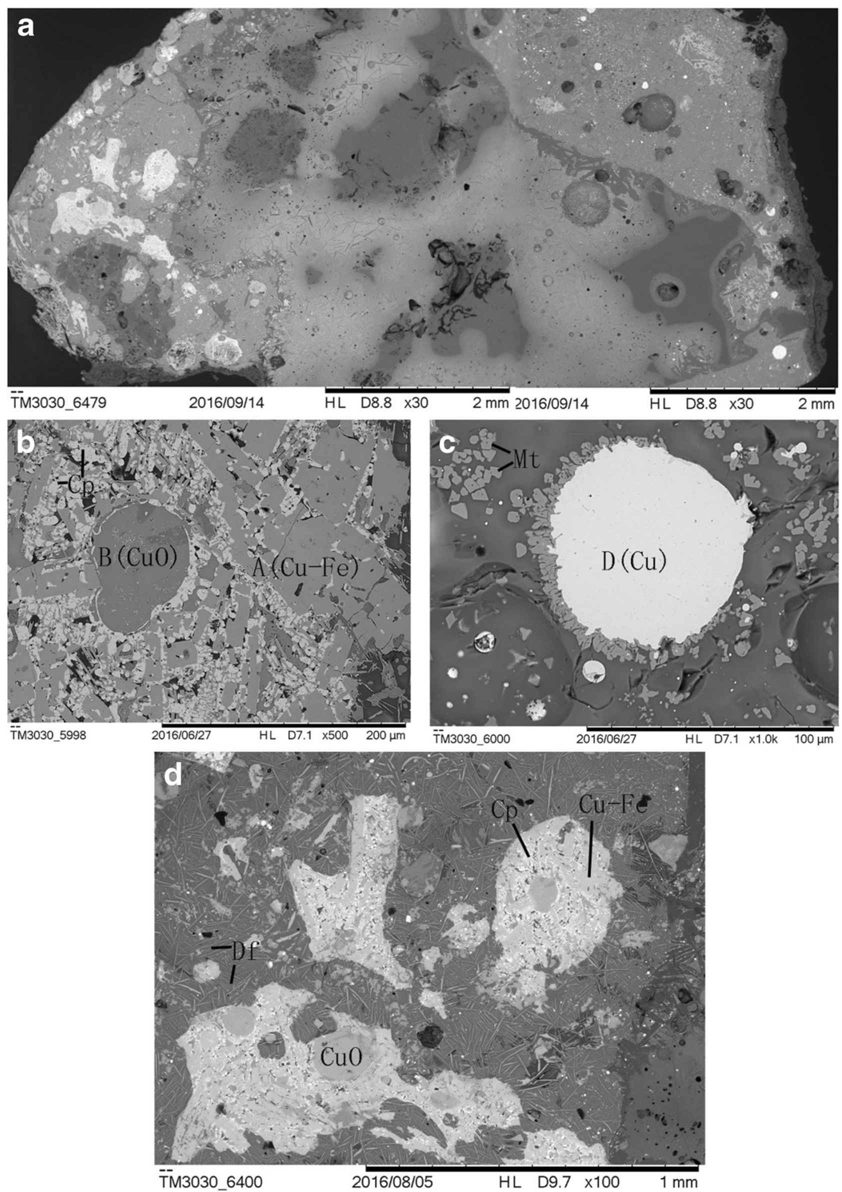

Fig. 10 BES images of GFT13 sample. showing that:**a**, the whole view BES image of the sample;**b**, Cp=cuprite;**c**, Mt=magenite;**d**, Cp=cuprite, Df= delafossite

smelting slag, cuprite and delafossite are usually treated as indicators of melting or refining slag formed under oxidizing conditions (Craddock 1995; Bachmann 1982). In some early smelting sites, the slags can also contain delafossite (Radivojevic et al. 2010; Müller et al. 2004). With reference to Fig. 10, point D indicates magnetite surrounding copper prill, while point A represents iron-rich copper, and point B indicates copper oxide. At all points, significant quantities of cuprite are also present, potentially indicating that iron was burned out from an initially iron-rich copper, such as in the case of iron-rich arsenical copper, as reported by Rehren and Liu (Rehren et al. 2012; Liu et al. 2015). More specifically, when iron-rich copper was burned, the iron formed iron oxide in addition to small quantities of magnetite. Similarly, Chakraborti and Lynch (1983) reported that the remelting of iron-rich arsenical copper under ambient conditions would immediately oxidize the iron, while the arsenic content would remain relatively constant until the majority of iron was removed from the alloy. Thus, upon refining, iron would be removed from the iron-rich copper species, as indicated upon moving from point A to point B in Fig. 10. However, due to the presence of a strong oxidizing atmosphere, the copper itself was also oxidized.

Refining is a relatively mature stage of copper metallurgy. From our results, it was clear that the GFT13 sample originated from the same stratum as GFT14, which we previously determined to have been excavated from the latest stratum among the various smelting slags, thereby indicating that both samples reflect a well-developed technological context.

Alloying slags

The results of previous studies showed that bronze alloying was achieved using one of four distinct techniques, namely, by remelting bronze scrap, through the addition of tin to copper or scrap bronze, by melting cassiterite with metallic copper, and by the co-smelting of a mixture of copper and tin (Cooke and Nielsen 1978; Dungworth 2000; Crew and Rehren 2002; Pigott et al. 2003; Renzi et al. 2007; Rovira 2007; Rovira et al. 2009; Figueiredo et al. 2010; Murillo-Barroso et al. 2010; Eliyahu-Behar et al. 2012; Valério et al. 2013a, b; Rademakers et al. 2013). Many more features, such as the copper content, the oxidizing conditions (as indicated by the phases present), and the physical appearance of the slag, should be considered to determine the method that was employed. The bulk chemical compositions of the melting slag matrices of the samples are outlined in Table 3, in which samples GFT5, GFT11, and CFT15 are all examples of a furnace wall-adhering slag.

As shown in Fig. 11a, GFT5 contains a large quantity of tin bronze prills. For example, two particles measuring approximately 1 and 2 mm in diameter have tin contents of 15.4 and 2.2%, respectively. In addition, the particle indicated at point C contains tin and copper contents of 40.8 and 57.7%, respectively.

In the matrix of the slag, significant quantities of cuprite and bronze particles were also present, although no iron oxide was detected, as the matrix is mainly composed of copper and tin. As the tin levels range between 2.1 and 40.8%, the sample appears to be alloyed using fresh tin and copper metal, as the tin content of the Dian period is generally <30%, as observed for the GFT11 sample. In addition, large quantities of copper prills were distributed within the furnace walls and the adhering slag of the GFT11 sample. Furthermore, a relatively large copper particle was observed (diameter = 500 μm) within the boundary region, in addition to various rectangular-, square-, and irregular-shaped SnO_2 prills along the edges of the particle. Tin bronze prills were also found in the slag, as was the case for the GFT15 sample.

In an oxidizing atmosphere, the metals in an alloy oxidize in sequence, according to their reactivities. In tin–copper alloys, tin is oxidized first. If a high level of oxidation is achieved, all of the tin in the alloy will be converted into oxide. Copper may also oxidize, although un-oxidized portions will remain. Hence, the tin bronze alloy prills found in the slag are unlikely to represent components of alloyed products, as the tin content has been decreased (Li and Hong 1995).

In Fig. 12a, the iron content of the sample GFT12 is approximately 0.5%. The dark gray section in the middle is copper oxide, with high levels of SnO_2. The matrix is mainly copper oxide. From Fig. 12b, c, we can see the presence of a large quantity of cuprite and SnO_2. This most likely formed by reoxidizing the metallic copper during the operation (Hauptmann 2007). The brightest area is very rich in rhomboidal cassiterite crystals, the diagnostic morphology of which is known to be derived from the oxidation of metallic tin (Dungworth 2000; Rovira 2007).

The composition of GFT20 is significantly different from those of the other examples of alloying slag, as its matrix contains around 35% iron, 14% copper, and 15% tin. The left side of the sample has comparatively few SnO_2 prills but more metallic copper prills. The right side has needle-shaped delafossites distributed throughout, as well as large numbers of tin bronze prills. In Fig. 13a, the largest particle is metallic copper, measuring around 300 μm. In Fig. 13b, the bronze particles measure around 200 μm, with cuprite close to them and large amounts of magnetite around them. In Fig. 13c, there are many cuprite prills, with magnetite and cassiterite distributed throughout the matrix. The phases indicate that the slag formed under a strong oxidizing atmosphere. Above, we have discussed the refining slag in GFT20. It has the characteristics of a refining slag, and the mount of cuprite prills indicates the melting of the slag.

Meanwhile, unlike GFT13, the iron content is much higher, with the FeO in the slag being >40%, indicating the addition

Table 3 Bulk chemical compositions of the melting slag matrices as determined by the SEM-EDS area analysis

Number	Scanned area	wt%										
		MgO	Al_2O_3	SiO_2	SO_3	K_2O	CaO	TiO	P_2O_5	FeO	CuO	SnO_2
GFT5	Left-hand area	1.8	3.0	19.9	n.d.	n.d.	5.5	n.d.	1.5	2.6	41.3	24.4
	Right-hand area	1.3	2.2	14.3	n.d.	n.d.	n.d.	n.d.	1.5	4.5	28.2	48.1
	Furnace wall	n.d.	7.9	72.7	n.d.	2.7	3.5	n.d.	n.d.	2.6	10.7	n.d.
GFT11	Furnace wall 1	2.3	3.8	27.6	n.d.	4.2	30.2	n.d.	19.9	6.9	5.2	n.d.
	Furnace wall 2	3.1	3.2	30.5	n.d.	2.9	24.3	n.d.	14.6	7.2	8.5	5.8
GFT12	Bright area on the left	n.d.	0.2	1.9	n.d.	n.d.	n.d.	n.d.	n.d.	n.d.	80.2	17.7
	Dark area in the middle	n.d.	1.3	40.2	n.d.	n.d.	2.1	n.d.	3.3	0.5	52.7	n.d.
GFT15	Furnace wall	1.0	2.0	40.0	n.d.	5.8	25.0	n.d.	16.0	5.0	5.3	n.d.
	Slag	3.3	3.2	25.7	n.d.	n.d.	12.3	n.d.	6.8	9.5	15.2	24.0
GFT20	Section 1	1.3	6.9	23.5	n.d.	n.d.	10.0	0.9	3.2	37.9	6.6	9.8
	Section 2	1.6	4.5	22.2	n.d.	n.d.	9.3	0.7	2.8	24.1	16.9	18.0

Data is presented in weight percent, normalized to 100

n.d. not detected

of another gangue. Thus, we can conclude that the tin is present as minteral tin.

The above characteristics exclude the possibility of bronze recycling, such that we can conclude that the Guangfentou site mainly used metal copper melting with cassiterite or mineral tin. It is very difficult to differentiate the type of tin that was used. Carlotta et al. (2017) studied slag samples from the Iberian Peninsula where the direct production of copper alloys was achieved by cementation and the co-smelting of mineral ores with feature elements from the mineral tin. Our experiments did not detect these feature elements. Even though the rhomboidal cassiterite crystals may be from the metallic tin, the tantalite in the slag indicates that the cassiterite entered the crucible in mineral form (Carlotta et al. 2017). In both of the samples, we can find the rhomboidal cassiterite crystals, but it is difficult to determine if the tin entered in mineral or metallic form. The presence of pseudomorphs of nodular cassiterite provides incontestable evidence that tin-bearing minerals were added to the charge, but they may not preclude the former's presence due to their having been

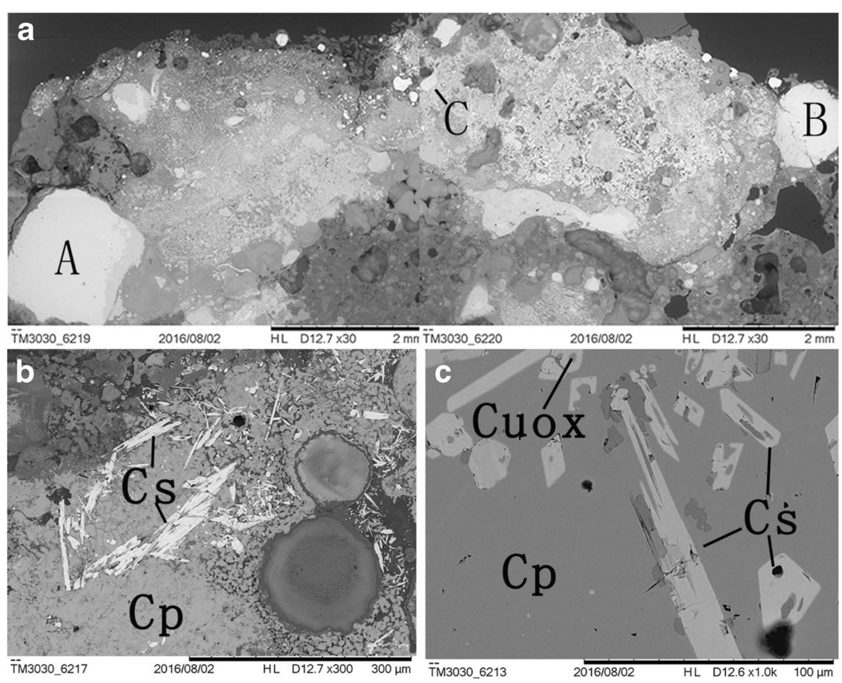

Fig. 11 BES images of GFT5 sample. showing that:**a**, the whole view BES image of the sample;**b**, Cs=cassiterite, Cp=cuprite;**c**, Cs=cassiterite

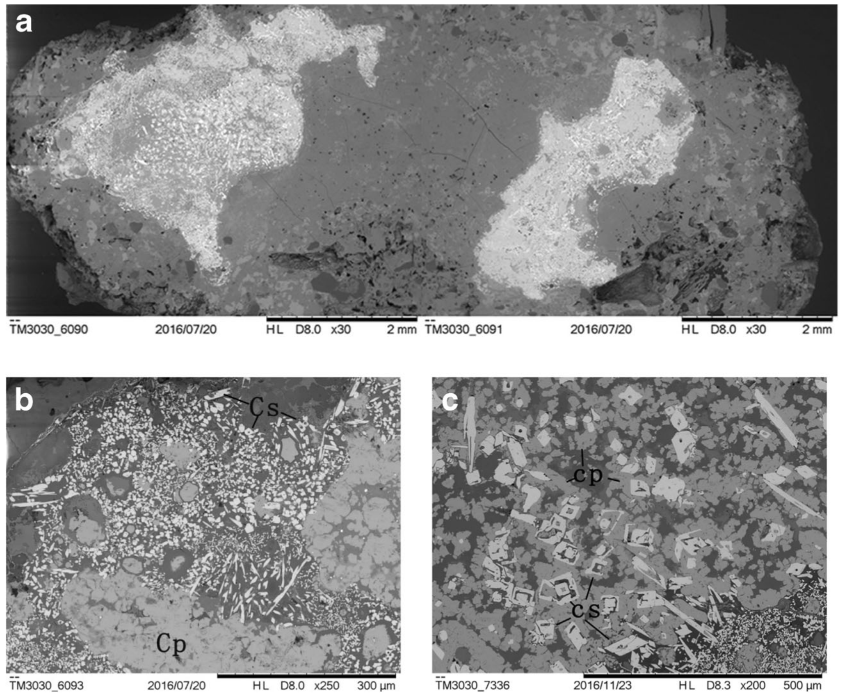

Fig. 12 BES images of GFT12. **a** The dark gray sections are copper oxide; **b** cp is cuprite and cs is cassiterite; **c** cp is cuprite and cs is cassiterite

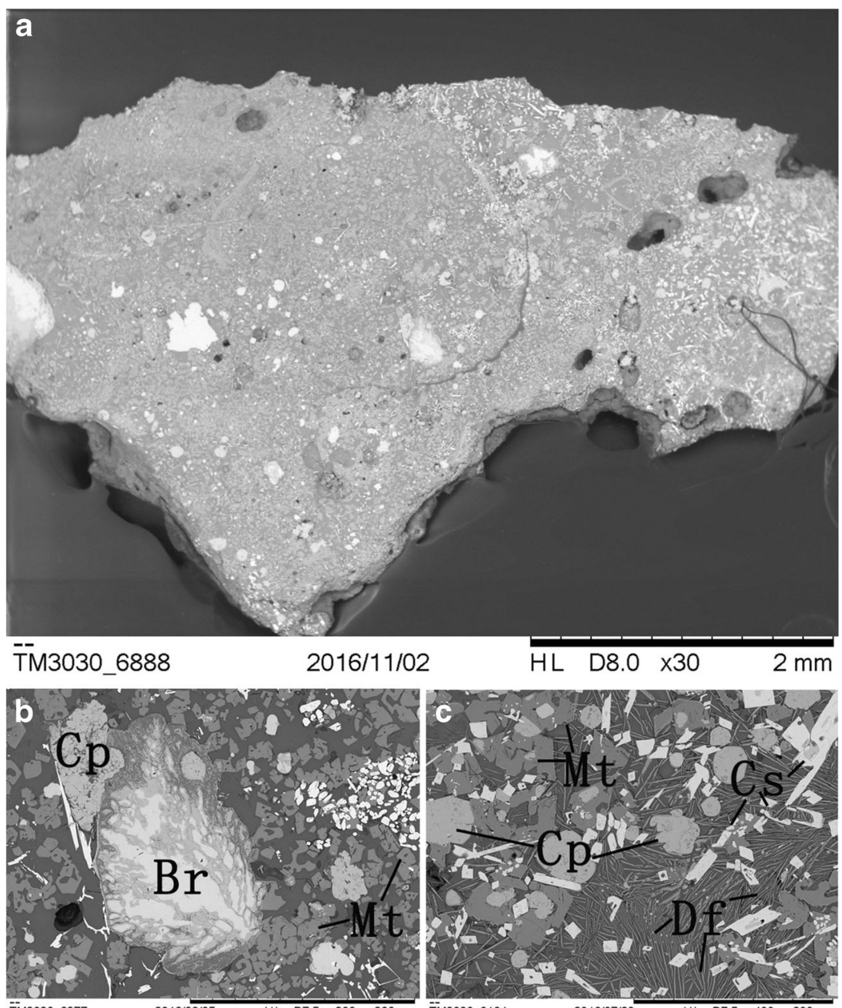

Fig. 13 BES images of GFT20. **a** Overall view of the sample; **b** *cp* cuprite, *Br* bronze, *mt* magnetite, *cs* cassiterite. **c** *cp* cuprite, *mt* magnetite, *df* delafossite, *cs* cassiterite

Table 4 Results of the SEM-EDS analyses on the metallic matrices as determined by the SEM-EDS area analysis

Sample number	Major elemental components (wt%)				
	Cu	Sn	S	Fe	Si
GFT3	100.0				
GFT4	98.8	1.1	0.1		
GFT9	100.0				
GFT19	99.7		0.2		0.1
GFT17	97.1	2.9			
GFT6	88.6	11.2	0.1		0.1
GFT16	75.6	23.0	0.1	1.0	0.3
GFT18	79.4	20.1	0.1		

Data is presented in weight percent, normalized to 100

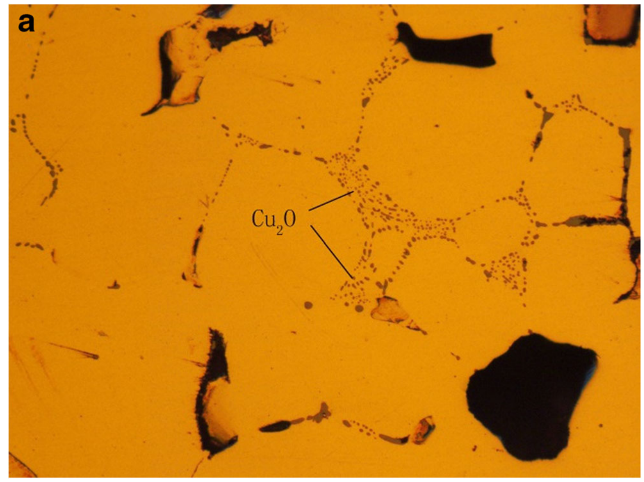

Fig. 14 Metallographic image of GFT9

reduced to metal and hence disappeared. (Rademakers et al. 2013; Carlotta et al. 2017). Both the alloying samples have an amount of tin oxide inclusions such as globular or euhedral needles, resulting from tin oxidation in the molten phase. The copper nucleus inside some of them suggests that both metals were under an oxidizing atmosphere, with the tin oxidizing to leave a metallic copper core (Dungworth 2000). Rovira (2004) believes that this is evidence of use of cassiterite.

From the SEM-BES of the alloying samples, all have rhomboidal cassiterite crystals, pseudomorphs of nodular cassiterite, and a copper nucleus inside tin oxide. But in GFT20, it may be concluded that it was the tin mineral added to the metal copper to the alloying bronze. We should, therefore, pay greater attention to the phases to determine the source of the tin.

Metallic copper

Ten different copper metal samples were employed for the purpose of this study, but GFT7 and GFT8 are very badly corroded, so we do not include them in the table; from the SEM-EDS detected, they both had low tin(<2%) and any materials containing 2 wt% (weight percent) of an element other than copper were treated as alloys (see Table 4). Thus, the GFT3, GFT9, and GFT19 samples were considered metallic copper, while the GFT6, GFT16, and GFT18 samples were classified as tin bronze alloys.

As indicated by the SEM-EDS analyses, GFT3 and GFT9 are copper metal, as no impurities were detected. More specifically, GFT3 contains large casted metallic copper α-phase solid-solution grains, while GFT9 is mainly composed of an α-phase solid solution, with ($\alpha + Cu_2O$) eutectic structures in its matrix distribution (Fig. 14). The presence of these eutectic structures indicates that solidification took place in a strongly oxidizing atmosphere during the copper melting process. According to the analyses of the slag samples, the refining of raw copper also takes place in a strong oxidizing atmosphere, and so, it may be the product of refining. In contrast, during the alloying process, GFT4 may be formed, as indicated by its increased degree of corrosion, and a small quantity of residual metal matrix. In addition, analysis of its composition indicated a low tin content in addition to a significant quantity of sulfide inclusions. Furthermore, in the GFT14 slag sample, small quantities of tin and sulfide were detected in the metal prills, suggesting that GFT4 is likely to be the product of the smelting GFT14 slag. Moreover, GFT19, GFT6, GFT16, and GFT18 contain small quantities of sulfide inclusions (Fig. 15), indicating that they are the products of smelting using sulfidic ores, while the GFT1 and GFT2 slags are produced from smelting sulfide ore, the copper which is particularly likely for late bronze alloying.

Through the analysis of different copper samples, it was apparent that the basic and slag samples examined herein are suitable for determining the products formed and the processes employed at the smelting sites. Smelting is performed

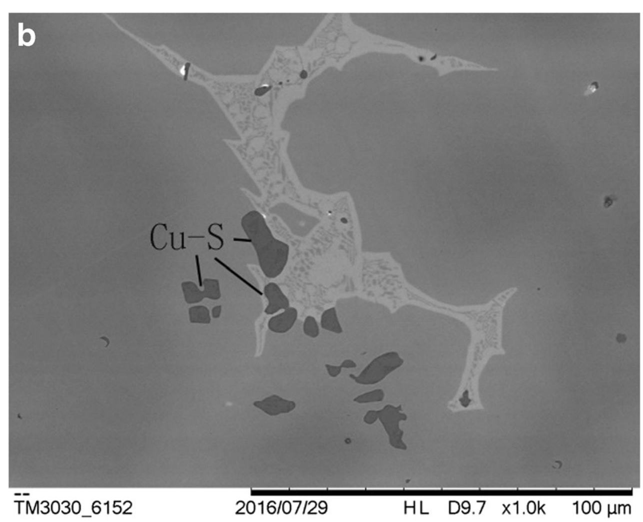

Fig. 15 BES image of GFT18

primarily on sulfide and oxide ores (mainly sulfide ores) to produce raw copper. Some of this raw copper is then melted with tin to obtain a tin bronze alloy, while the other portion is refined to obtain metallic copper, which is then melted with other metals in a specific ratio to produce bronze. In addition, some of the produced copper may be cast into ingots for export, while other portions may be alloyed with lead to form lead bronze alloys according to the needs at that time, although we have yet to discover bronze artifacts contain lead. Stone molds were unearthed at the Guangfentou site, thereby indicating the capability to produce cast artifacts. As previously mentioned, the slags were found in the second stage of the early civilization layer, alongside many earthen artifacts. In addition, housing facilities and large ash pits were discovered, indicating that this was a well-equipped copper smelting and casting site, with its main products being metallic copper and tin bronze.

Connections with the Dian civilization

Bronze casting ruins in the Central Plains are primarily distributed in political centers and their surrounding regions (Wang 2013) at a considerable distance from copper mineral resources. This includes examples such as Erlitou in the Yanshi county (Joint Archaeological Team of IA and CASS 1999), the Zhengzhou Shang City (Henan Provincial Institute of Cultural Relics and Archaeology 1987), Yinxu in the Anyang prefecture (Joint Archaeological Team of IA and CASS 1987), Beiyao in Luoyang City (Luoyang Cultural Relics Task Force 1983), Zhouyuan in the Shaanxi province (Zhouyuan archaeological team 2004), the ancient city of Zhenghan in the Xinzheng county (The Xinzheng workstation of Henan Provincial Museum 1980), and Xintian, the ancient capital of the Jin state (Shanxi Provincial Institute Of Archaeology 1993). The main reason for this configuration is to satisfy the demands of the royal aristocracy for bronze and to give them control of this important resource.

As such, bronze casting ruins are generally found close to important regions, and so, correspondingly, important housing relics are frequently encountered nearby. For example, the Guangfentou site is only about 10 km from the well-known Lijiashan ancient cemetery, which dates back to the Dian Kingdom on the northwest coast of the Fuxian Lake. The tombs were discovered in 1966, with excavation commencing in 1972. A total of 27 tombs have been excavated, and over 1000 bronze artifacts have been unearthed, which account for >80% of the funerary objects discovered (Zhang and Wang 1975). In addition, Li et al. (2008) analyzed the compositions of 45 artifacts from the Lijiashan cemetery and found that tin bronze alloys account for 57.8% of the artifacts, which were primarily used in weapons and production tools. Among the eight artifacts that were listed in the corresponding publication, six were tin bronze alloys with tin contents ranging from 10 to 20%. Indeed, tin bronze alloys compose a large proportion of the Jiangchuan Lijiashan cemetery. Cui and Wu (2008) also analyzed the compositions of seven artifacts by X-ray fluorescence and found that four artifacts were bronze products, one artifact had a low lead content, one was a bronze drum, and the final artifact was a copper stove with a relatively high lead content. Combined with Li and Cui's experimental data, in terms of the alloy ratios, the weapons, farm tools, decorations, and other tin bronze- and copper-based artifacts essentially contained no lead. In contrast, early large bronze drums and tin bronze-based copper shell storage containers had medium to high quantities of lead. It is generally believed that lead–tin bronze is a higher stage of bronze culture, i.e., the tin bronze technology is a more mature technology. Indeed, all melting slags analyzed herein were melted tin bronze samples. Based on our previous analyses of the metallic copper blocks, it seems likely that they were among the raw materials used to adjust the tin-to-copper ratio in tin bronze artifacts. The tin contents of the tin bronze alloys are also mostly in the range of 10–20%, which is consistent with the artifacts found at the Lijiashan cemetery. However, in the GFT10 sample, large numbers of lead prills exist in the copper prills, indicating that the low-lead-content tin bronze artifacts are smelted from the lead-containing copper ores. Furthermore, no lead-containing slags or metals were found, indicating that the Guangfentou ruins can be considered early ancient Dian culture relics.

The use of lead isotopes was proposed by Brill and Wampler (1965) and Grögler et al. (1966) for application as part of an investigation using mounts, a well-established method for determining the provenance of a raw material (Pollard and Heron 2008; Villa 2009). Lead has four stable isotopes, namely, ^{204}Pb, ^{206}Pb, ^{207}Pb, and ^{208}Pb, and the measurement of their isotopic ratios can allow the calculation of the geological age of the lead minerals. In the 1980s, Jin (2008) began to study lead isotopes and suggested that the presence of high radiogenic lead in the bronze medals of the Shang dynasty may be related to resources in the northeastern part of Yunnan. Li (2000) also used lead isotope analysis to examine bronze samples from Yunnan, while Cui and Wu (2008) detected and discussed the lead isotopic ratios present in 83 ancient bronze samples unearthed in Yunnan and Vietnam in the context of the ancient Dian culture.

The Guangfentou site lead isotopic ratios measured are shown in Table 5. From the lead isotope scatter diagram shown in Fig. 16, it is apparent that the Guangfentou samples are distributed over a relatively large area, indicating that the ores were sourced from diverse areas, as discussed above. In addition, the smelting technology employed on this site remained relatively constant over a long period of time, and it appears that the metallurgical craftsmen of this site had access to a wide range of ores. The lead isotope ratios of the Guangfentou slags were then compared with those of the

Table 5 Lead isotopic ratios measured on the metallurgical relics from the Guangfentou ruins

Sample number	207/206	208/206	206/204	207/204	208/204
GFT1	0.860548	2.112454	18.15708	15.62374	38.35598
GFT2	0.839246	2.083635	18.59161	15.60461	38.74129
GFT3	0.848171	2.098734	18.39141	15.60327	38.59869
GFT4	0.829093	2.090995	18.834	15.61574	39.38244
GFT6	0.844785	2.097146	18.49516	15.62549	38.78738
GFT8	0.828674	2.069912	18.86917	15.63649	39.05738
GFT9	0.860683	2.100448	18.17649	15.64419	38.17877
GFT10	0.846246	2.088488	18.42957	15.59605	38.49021
GFT13	0.837795	2.060898	18.71828	15.68442	38.58255
GFT14	0.850588	2.119771	18.33426	15.5949	38.86443

Shizhaishan-type bronze drums. As indicated in the figure, the isotope ratio distributions of the two overlap slightly, indicating that the bronze drum ore originated from the Guangfentou site. Furthermore, three of the four copper artifacts unearthed at the Lijiashan tombs contained lead isotope ratios that fell within the distribution range of the Guangfentou slags, indicating a close relationship between the sources of ore used in the two sets of relics. It therefore appears that the Guangfentou site is likely to be the site where the copper artifacts of the Lijiashan- and Shizhaishan-style bronze drums were cast or the origin from which the raw materials used to create these relics were sourced.

Furthermore, flotation analyses of plant remains from the Guangfentou site show that the main agricultural crops at this site were wheat, rice, and foxtail millet, with hull-less barley and proso millet being used as supplementary crops. Agricultural products from the northwest were also found in

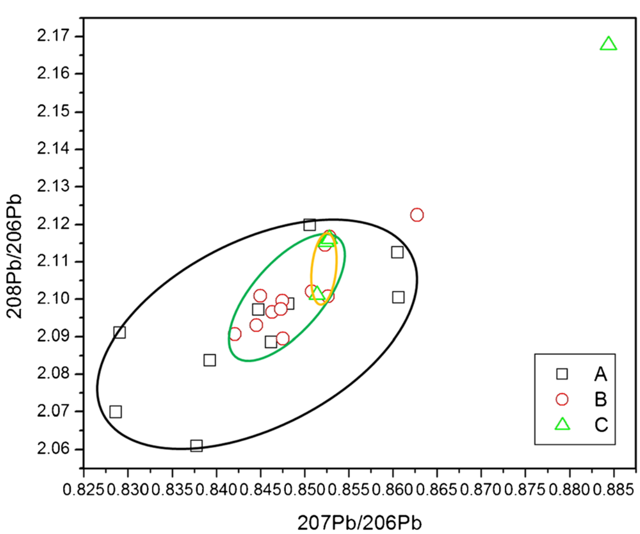

Fig. 16 Lead isotope ratios of the slags obtained from the Guangfentou site (*A*), Shizhaishan-type bronze drums (*B*) (Wei et al. 2002; Cui and Wu 2008), and copper artifacts unearthed from the Lijiashan tombs (*C*) (Cui and Wu 2008)

balanced proportions. It is therefore likely that the mixed farming of rice and millet provided a safeguard for the development of handiworks at this site (Li and Liu 2016), while also providing a material basis for the smelting and casting of bronze in this region.

Conclusions

The study of metallurgical relics is important in understanding the origins of Bronze Age civilizations in Yunnan, China. The nature of the Guangfentou site in Jiangchuan, Yunnan, can be determined via the unearthing and analysis of metallurgical relics. These metallurgical relics can be categorized into slags and copper/bronze metallic, with the former being composed of smelting and melting slags. Smelting slags are obtained from the smelting of sulfidic ores and tin-containing oxide ores, but we have yet to precisely determine the complete set of smelting processes that were used at the site. In contrast, melting slags include refining slags and alloying slags, where examples of alloying slags mainly used metallic copper with tin; it can be concluded that the tin mineral was used. But it is very difficult to differentiate what other kind of tin was used. Stone molds were also unearthed at this site, and there are some artifacts which were unearthed, which implied that the site can also cast and construct copper and bronze artifacts.

Lead isotope analysis is also an important method to determine the origins of ore samples. In this work, the lead isotope ratios of slags from the Guangfentou site and of the Shizhaishan-type bronze drums and copper artifacts unearthed at the Lijiashan site were compared. The lead isotope ratios of the slags and copper artifacts obtained from the Guangfentou site partly overlapped with the known lead isotope ratio distributions of the Shizhaishan-type bronze drums and the copper artifacts unearthed from the Lijiashan tombs. This indicates that the three sites likely employed the same sources of ore at a certain time, which is important information in the determination of ore sources for the Shizhaishan-type bronze drums and the Dian civilization bronze artifacts. Our analysis therefore indicates that Guangfentou site is likely be the production site or source of unearthed copper artifacts from the Lijiashan tombs.

To date, few studies have been performed on early Yunnan smelting sites, and the Guangfentou site is currently the only known and studied Dian civilization site where smelting, melting, and casting were performed simultaneously. In addition to providing information on the Guangfentou site itself, this work has significant implications for studies into early metallurgical relics from Yunnan, investigations into early Bronze Age civilizations in Yunnan and Southeast Asia, and the propagation of culture, knowledge, and interaction between these civilizations.

Acknowledgements This research was supported by the National High-Level Personnel Special Support Program (Ten Thousand Talents Program), the "Young Talents Program" sponsored by the Beijing City School of Higher Education, and the National Social Science Fund (project approval number 15ZDB057, "Research on Porcelain Exported from Ancient China Unearthed in Africa and the Maritime Silk Road"). We would also like to thank Professor Li Yanxiang and Dr. Liu Siran from the University of Science and Technology, Beijing for their guidance in our experiments and the process of writing this paper. We also thank Professor Wu Xiaohong and Senior Engineer Huang Baoling from Peking University for their support during this study.

References

Allard F (1998) Stirrings at the periphery: history, archaeology and the study of Dian. Antiquity 2(4):321–341

Avetisyan HK (1954) Metallurgiya chernovoi medi. Moscow, Metallurgiya, pp 1–464 (in Russian)

Bachmann HG (1982) The Identification of slags from archaeological sites. Institute of Archaeology, London

Brill RH, Wampler JM (1965) Isotope studies of ancient lead. Am J Archaeol 69:165–166

Carlotta F, Martinón-Torres M, Álvarez DG (2017) Bronze production in the Iron Age of the Iberian Peninsula: the case of El Castru, Vigaña (Asturias, NWSpain). J Archaeol Sci Rep 11:338–351

Chakraborti N, Lynch DC (1983) Thermodynamics of roasting arsenopyrite. Metallurgical Tansactions B 14B:239–251

Cooke SRB, Nielsen BV (1978) Excavations at Nichoria in Southwest Greece site, environs and techniques Vol. 1. In: Rapp G Jr, Arschenbrenner SE (eds) Slags and other metallurgical products. University of Minnesota Press, Minneapolis, pp 182–224

Craddock PT (1995) Early metal mining and production. Edinburgh University Press, Edinburgh

Crew P, Rehren T (2002) High-temperature workshop residues from Tara: iron, bronze and glass. Discov Program Rep 6:83–103

Cui JF, Wu XH (2008) The study of lead-isotope archaeology: provenance study of bronze artefacts unearthed from Yunnan Province, China and Vietnam. Cultural Relics Press, Beijing(in Chinese)

Dungworth D (2000) Serendipity in the foundry? Tin oxide inclusions in copper and copper alloys as an indicator of production process. Bull Metals Mus 32:1–5

Eliyahu-Behar A, Yahalom-Mack N, Shilstein S, Zukerman A, Shafer-Elliott C, Maeir AM, Boaretto E, Finkelstein I, Weiner S (2012) Iron and bronze production in Iron Age IIA Philistia: new evidence from Tell es-Safi/Gath. Israel J Archaeol Sci 39:255–267

Figueiredo E, Silva RJC, Senna-Martinez JC, Fatima Araujo M, Bras Fernandes FM, Ines Vaz JL (2010) Smelting and recycling evidences fomthe Late Bronze Age habitat site of Baioes (Viseu, Portugal). J Archaeol Sci 37:1623–1634

Grögler N, Geiss J, Grünenfelder M, Houtermans FG (1966) Isotopenuntersuchungen zur Bestimmung der Herkunft römischer Bleirohre und Bleibarren. Z Naturforsch 21a:1167–1172

Hanning E, Gauss R, Goldenberg G (2010) Metal from Zambujal: experimentally reconstructing a 5000-year-old technology. Trab Prehist 67:287–304

Hauptmann A (2003) Archaeometallurgy in Europe. Proceedings International Conference. In: Rationales of liquefaction and metal separation in earliest copper smelting: basics for reconstructing Chalcolithic and Early Bronze Age smelting processes. Associazione Italiana Metallurgia, Milan, pp 459–468

Hauptmann A (2007) The archaeometallurgy of copper. Springer Berlin, Heidelberg, 103(2):423–424

Henan Provincial Institute of Cultural Relics and Archaeology (1987) The cast copper base of Erligang in the Shang dynasty in Zhengzhou. Cultural Relics Press, Beijing(in Chinese)

Hohlmann B (1997) Beitrag zur spätbronzezeitlichen Kupfermetallurgie in Trentino(Südalpen) im Vergleich mit anderen prähistorischen Kupferschlacken aus dem Alpenraum. Faculty of Geosciences, Ruhr-University Bochum, PhD dissertation

Jiang ZL,Zhu ZH (2014-01-03) An important achievements of archaeological excavation in YuBeidi site in Dongchuan,Yunnan province. China Cultural Relics News (in Chinese)

Jin ZY (2008) Lead isotope archaeology in China. China University of Science and Technology Press, Hefei (in Chinese)

Joint Archaeological Team of IA, CASS (1987) A report of 1958–1961 in Yinxu site. Cultural Relics Press, Beijing (in Chinese)

Joint Archaeological Team of IA, CASS (1999) A report of 1959–1978 excavation in Erlitou site in Yanshi. Encyclopedia of China Publishing House, Beijing (in Chinese)

Li XC (2000) Chinese lead isotope archeology. Yunnan Science Press, Kunming (in chinese)

Li YX (2007) A preliminary study on Erlitou Bronze foundry site. Archaeology of science and technology. Technology & Technical Publisher, Beijing (in Chinese)

Li XR 2016–6-31. The achievements of archaeological excavation in Guangfentou site ,Jiangchuan,Yunnan province. Chinese Cultural Relics News(in Chinese)

Li XC, Han RB (2011) The ancient Dian kingdom metal technology research. Science Press, Beijing (in Chinese)

Li YX, Hong YR (1988) Slagery of copper smelting in antiquity. Sci Conserv Archaeol 1:28–34 (in Chinese)

Li YX, Hong YR (1995) Slagery of copper smelting in antiquity. Sci Conserv Archaeol 1:28–34 (in Chinese)

Li XR, Liu X (2016) An analysis on the carbonized seeds and fruits from Guangfentou site in Jiangchuan, Yunnan. Agricul Archaeol 3:20–27 (in Chinese)

Li XC, et al. (2008) Scientific analysis of metal artefacts unearthed in the Lijiashan ancient tomb , Jiangchuan, Yunnan Province. Archaeol.8: 76–90(in Chinese)

Liu S, Thilo R, Pernicka E, Arnulf Hausleiterka E (2015) Copper processing in the oases of northwest Arabia: technology, alloys and provenance. J Archaeol Sci 53:492–503

Luoyang Cultural Relics Task Force (1983) Excavation of casting ruins in Western Zhou Dynasty in Beiyao. Luoyang Archaeol 08:430–441 (in Chinese)

Min RWJ (2009) The excavation briefing in Yinsuo Island, Haidong, Yunnan province. Archaeol 08:23–41 (in Chinese)

Müller R, Rehren T, Rovira S (2004) Almizaraque and the early copper metallurgy of southeast Spain: new data. Madr Mittl 45:33–56

Murillo-Barroso M, Pryce M, Bellina TO, Martinón-Torres M (2010) Khao Sam Kaeo—an archaeometallurgical crossroads for trans-asiatic technological traditions. J Archaeol Sci 37:1761–1772

Pigott VC, Rogers HC, Nash SK (2003) Archaeometallurgical investigations at Malyan: the evidence for tin-bronze in the Kaftari Phase. In: Miller NF, Abdi K (eds) Yeki Bud, Yeki Nabud: Essays on the archaeology of Iran in honor of William M. Sumner. Cotsen Institute of Archaeology at UCLA, Los Angeles, pp 161–176

Pollard AM, Heron C (2008) Archaeological chemistry. Royal Society of Chemistry, Cambridge

Qi LL (2014) Study of the remains of smelting site in Shijiazhai in Jinping of Yunnan. University of Science and Technology Beijing, Beijing (in Chinese)

Qiu RR 2015-10-14. Excavation of Bronze Age remains of Dian in Xingyi Site, Yunnan Province. Yunnan Daily(in Chinese)

Rademakers FW, Rehren T, Pusch E (2013) Bronze production in Pi-Ramesse: alloying technology and material use. In: Ben-Yosef E, Goren Y (eds) Mining for copper: essays in honor of Professor Beno Rothenberg. Institute of Archaeology of Tel Aviv, Tel Aviv (in press)

Radivojevic M, Rehren T, Pernicka E, Sljivar D, Brauns M, Boric D (2010) On the origins of extractive metallurgy: new evidence from Europe. J Archaeol Sci 37:2775–2787

Rehren T, Boscher L, Pernicka E (2012) Large scale smelting of speiss and arsenical copper at Early Bronze Age Arisman, North-West Iran. J Archaeol Sci 39:1717

Renzi M, Hauptmann A, Rovira S, (2007) Phoenician metallurgical production at S-E Spain. Proceedings of the 2nd International Conference "Archaeometallurgy in Europe 2007", Grado-Aquileia [CD-ROM]

Rovira S (2004) Tecnología metalúrgica y cambio cultural en la Prehistoria de la Península Ibérica. Norba Revista de Historia 17: 9–40

Rovira S (2007) La producción de bronces en la prehistoria. In: Molera J, Farjas J, Roura P, Pradell T (eds) Avances En Arqueometría, Actas Del VI Congreso Ibérico De Arqueometría, vol 2005. Universidad de Girona, Girona, pp 21–35

Rovira S, Montero-Ruiz I, Renzi M (2009) Experimental co-smelting to copper-tin alloys. In: Kienlin TL, Roberts BW (eds) Metals and societies. Studies in Honour of Barbara S. Ottaway.Universitatsforschungen zur prahistorischen Archaologie. R.Habelt, Bonn, pp 407–414

Ryndina N, Indenbaum G, Kolosova V (1999) Copper production from polymetallic sulphide ores in the Northeastern Balkan Eneolithic culture. J Archaeol Sci 26:1059–1068

Shanxi Provincial Institute Of Archaeology (1993) The Houma bronze foundry site. Cultural Relics Press, Beijing (in Chinese)

The Xinzheng workstation of Henan Provincial Museum (1980) Drilling and excavation of Zhenghan Old City in Xinzheng, Henan province. Cultural Relics Press, Beijing (in Chinese)

Tylecote RF (1980) Copper ingots and marine copper. Int J Naut Archaeol 9(1):67–68

Tylecote RF (1982) Early metallurgy in Cyprus. In: Muhly JD, Maddin R, Karageorghis V (eds) The Late Bronze Age: copper and bronze metallurgy at Enkomi and Kition. 4000–500 B.C.Pierides Foundation, Nicosia, pp 81–103

Tylecote RF and Boydell PF (1978) Experiments on copper smelting in chalcolithic copper smelting. Institute for Archaeometallurgy Studies, London

Valério P, Monge Soares AM, Silva RJC, Araújo MF, Rebelo P, Neto N, Santos R, Fontes T (2013a) Bronze production in southwestern Iberian Peninsula: the Late Bronze Age metallurgical workshop from Entre Águas 5 (Portugal). J Archaeol Sci 40:439–451

Valério, P., Monge Soares, A.M., Silva, R.J.C., Araújo, M.F., Rebelo, P., Neto, N., Santos, R.,Fontes, T., 2013b. Bronze production in southwestern Iberian Peninsula: the Late Bronze Age metallurgical workshop from Entre Águas 5 (Portugal) J Archaeol Sci 40, 439–451

Villa IM (2009) Lead isotopic measurements in archeological objects. Archaeol Anthropol Sci 1:149–153

Wang K (2013) Preliminary study on bronze casting ruins of Shigudun site in Tongling. Peking University, Beijing (in Chinese)

Wang DD, Sun SY, Li Y (1997) Investigation on slag smelting sites and analysis of slag in Gejiu, Yunnan province. Cult Reli Cent China 2: 104–107 (in Chinese)

Wei DP, Fang M, Wan F (2002) Abundant concentration of lead on the sample of bronze drum in Viet Nam and Survey for Lead isotopic. J Guangxi Univ Natl (Nat Sci Ed) 04:7–59 (in Chinese)

Yang F (2010) Archaeology of ancient Yunnan of 1979–2009. Yunnan People's Publishing House, Kunming (inChinese)

Zhang ZQ (1989) Bronze cultures in Yunnan province. Ethn Art Stud S1: 59 (in Chinese)

Zhang ZZ (2000) History of metallurgy in Yunnan province. Yunnan Fine Arts Publishing House, Kunming (in Chinese)

Zhang Z, Wang D (1975) Excavation of an ancient cemetery at Li-Chia-Shan in Chiang-Ch'uan county, Yunnan Province. Acta Archaeol Sinica 2:97–156 (in Chinese)

Zhouyuan archaeological team (2004) The discovery of Western Zhou Dynasty tombs and bronze ruins at Zhouyuan site. Archaeol. 01, 3–6(in Chinese)